

# Metamorphic epitaxial materials

Christopher J.K. Richardson and Minjoo Larry Lee,  
Guest Editors

Mechanisms of dislocation generation and methods of crystal growth are two historically rich areas of scientific study. These two fields converge in the area of metamorphic epitaxial materials, where the goal is to produce high-performance devices that contain high densities of crystal defects in regions of the engineered material away from the active areas. Metamorphic epitaxy is a form of thin-film growth, where the lattice structure of the layer and substrate are mismatched, and its defining characteristic is that any elastic strain in the overlayer has been relaxed by the deliberate introduction of dislocations at the film–substrate interface. Metamorphic growth enables novel combinations of relaxed single-crystal materials to realize novel functionality and performance in numerous technological areas, including lasers, photovoltaics, transistors, and quantum computing. Many of the devices described in this issue are impossible to realize using the traditional approach of avoiding dislocation generation; instead, they rely on metamorphic epitaxy to attain high performance.

## Introduction

The desire to have complete deterministic control over composition and structure is a guiding passion for many materials engineers and scientists. Those who grow epitaxial materials have mastered the technique to such a degree that by following a general set of rules, certain combinations of atoms can be combined with a high level of confidence into a predetermined lattice of a stratified material with very few dislocations. These relatively defect-free, single-crystal epitaxial heterostructures are made into a variety of devices found in cell phones, computers, and light sources, among others, that undoubtedly play a central role in modern-day life. The performance of all electronic and optoelectronic systems, circuits, and devices, whether for computation, communication, sensing, or energy conversion, are limited by the properties of the constituent materials. For some applications, bending the rules of epitaxial growth is necessary to attain the next level of performance. One example is the efficiency improvements in metamorphic multijunction solar cells, where deviating from a single lattice constant allows the device designer to choose absorber materials with a wider range of bandgap values to more optimally divide the solar spectrum.

The term “metamorphic epitaxial material” describes a single-crystal thin film on a single-crystal substrate, where the film and substrate have a significant structural difference. This difference is often the relative lattice constants of the film and

substrate, but can also include film/substrate materials with different unit cells. The term metamorphic is similar to the geological and biological designation indicating a “change in form,” because there is indeed a change in the material structure due to the elastic strain relaxation and plastic deformation processes that occur during the growth process. By transcending the conventional paradigm of lattice-matched crystal growth in epitaxy, an emerging class of engineered materials is enabling devices to reach new performance levels. As illustrated schematically in **Figure 1**, lasers, transistors, solar cells, and even quantum computer components of the future are a few examples of these emerging metamorphic materials described in this issue of *MRS Bulletin*.<sup>1–4</sup>

## Epitaxial growth paradigms

Epitaxial growth paradigms can be generally grouped under three classes: homomorphic, pseudomorphic, and metamorphic.<sup>5</sup> These growth paradigms are briefly reviewed, as all three are widely employed in modern heterostructures.

Homomorphic growth, or homoepitaxy, is the first category, both because of its historic significance in the development of epitaxial crystal growth and surface science and because of its relative simplicity. Homomorphic epitaxy is the growth of a single-crystal thin film on a single-crystal substrate that is composed of the same material. The single-crystal substrate acts as the seed crystal that enables the growth of a coherent

Christopher J.K. Richardson, Laboratory for Physical Sciences, University of Maryland, USA; richardson@lps.umd.edu  
Minjoo Larry Lee, Department of Electrical Engineering, Yale University, USA; minjoo.lee@yale.edu or milee@alum.mit.edu  
DOI: 10.1557/mrs.2016.7

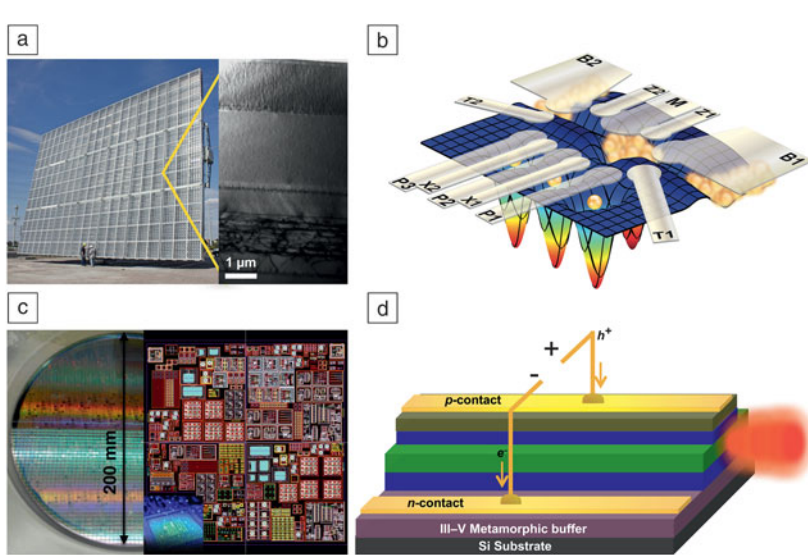


**Figure 1.** Examples of both near- and long-term applications of metamorphic epitaxial materials. (a) High-concentration photovoltaic system. Inset: bright-field transmission electron microscope image of an ultrahigh-efficiency metamorphic triple-junction GaInP/GaInAs/Ge solar cell showing (top to bottom), the GaInP top cell, GaInAs middle cell, and graded buffer region. Adapted with permission from Reference 33. (b) Quantum computing. Schematic diagram of a triple-dot device depicting the gate layout and the resulting electrostatic control of the potential landscape (colored contours). Electrons are schematically depicted as yellow spheres, and are provided by a 2D electron gas formed in strained Si grown on metamorphic SiGe on Si. The lateral triple dot is formed underneath gates labeled P1, P2, and P3. Gates X1 and X2 affect the tunnel coupling (exchange) between dots P1 and P2, and dots P2 and P3, respectively. A local charge-sensing quantum dot is formed under the gate labeled M, whose tunnel rates to the bath are controlled by gates Z1 and Z2. Adapted with permission from Reference 1. © 2015 AAAS. (c) Advanced electronics. (Left) 200-mm III-V/Si wafer, and (right) 20 mm × 20 mm chip layout where III-V and Si components are seamlessly integrated to enable new functionality. Inset shows a notional electronic/photonic chip. (d) Optoelectronic and photonic integration. Schematic diagram of metamorphic III-V on Si laser, a potential enabler for Si photonics and novel sensing platforms.

overlayer (i.e., no broken bonds at the interface). Because the film and substrate are identical, the two are perfectly lattice matched with zero misfit strain. The ability to grow high-quality homomorphous materials is important from a technological perspective, because changes in doping (e.g., *p*-type, *n*-type) along the growth direction can be used to create functionality, such as *p*–*n* junction diodes or *n*–*p*–*n* bipolar junction transistors. Additionally, homoepitaxial layers are extensively used as buffer layers to bury residual contamination from the substrate surface prior to device growth.

The second paradigm, pseudomorphic growth (e.g., InGaAs on GaAs) or lattice-matched heteroepitaxy (e.g., AlGaAs on GaAs), is the growth of a single-crystal film on a single-crystal structure composed of different materials, but with fully coherent atomic bonds. The freedom to engineer the alloy composition of the epitaxial layer directly led to the demonstration of the double heterostructure laser,<sup>6–8</sup> high-brightness visible light-emitting diodes (LEDs),<sup>9</sup> and numerous other semiconductor devices of commercial significance.<sup>5,10</sup> However, in order to maintain a fully coherent crystal structure that is not highly defective, the epitaxial layers must be chosen to maintain similar crystal structures and nearly identical lattice

constants to that of the substrate; they must reside on a nearly vertical line (see Figure 2). For strained layers, there is a critical thickness beyond which the formation of misfit dislocations becomes energetically favorable. The misfit dislocations allow the layer to relax by plastic deformation. This can greatly reduce the technical value of materials in both electronic and optoelectronic applications if care is not taken. Most pseudomorphic layers are designed to be as lattice matched as technically possible with residual misfit strains below 0.1%; but thin strained layers with misfit strain of approximately 1% are often designed as quantum wells and conduction channels.

The limitation of nearly lattice-matched materials drove early device designers to develop quaternary alloys (e.g., GaInAsP, AlGaInAs), such that the bandgap could be varied over a wider design space without changing the lattice constant; quaternary alloys are critical to the operation of telecommunication devices grown on InP substrates.<sup>10</sup> Today, state-of-the-art lasers reported in the scientific literature include quinary alloys, which have up to five III–V compound semiconductor elements, to enable engineered control of the lattice constant, bandgap, and the valence-band offset.<sup>11,12</sup> Device designers are also increasingly looking to further manipulate semiconductor band extrema by deliberately growing heavily strained layers that may have elastic strain approaching 3%.

However, this is an extremely challenging

approach because layers with this amount of strain are on the edge of stability; to remain dislocation free, these layers can only be grown a few monolayers thick.<sup>13</sup> The use of increasing numbers of alloy components and highly strained layers with critical thickness on the order of monolayers demonstrates the desire to increase the degree of freedom that can be employed to produce enhanced epitaxial materials.

The third growth paradigm, and the subject of this issue of *MRS Bulletin*, is metamorphic epitaxial growth or growth of fully relaxed, lattice-mismatched materials. Metamorphic layers are grown thicker than the critical thickness that limits design grown within the pseudomorphic paradigm. In metamorphic systems, there is, in principle, no limit to the degree of lattice mismatch that can be accommodated. Early studies in this area found that misfit dislocations that accommodate the lattice mismatch between an epitaxial layer and substrate often generate threading dislocations.<sup>14</sup> Since dislocations cannot terminate within crystals (unless as a loop), threading dislocations that terminate at the film surface are typically “left behind” from the relaxation process. Threading dislocation density (TDD) is generally determined by the kinetics of dislocation nucleation and glide, as threading

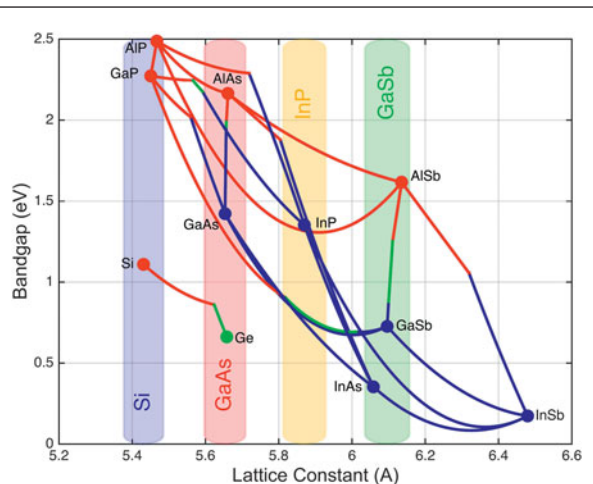


**Figure 2.** Graph displaying the bandgaps and lattice constants of III–V compound semiconductor and silicon-germanium alloys. Dots and line segments that are blue indicate direct-gap materials. Indirect materials with sixfold conduction-band symmetry are shown in red, and materials with eightfold conduction-band symmetry are shown in green. The vertical colored bars represent common commercial substrates. The width of each bar represents the range of lattice constants that produce up to 1% strain, indicating the range of alloys that can be grown nearly lattice matched. Without metamorphic growth, the conventional pairing of substrates and epitaxial layers that are vertically aligned necessitates a variety of substrate materials in order to design devices with different bandgaps.

dislocation segments contribute relatively little to strain relaxation; threading dislocations are often nearly vertical, and the amount of strain relieved by a dislocation is proportional to its length projected onto the interface plane. Since they act as nonradiative recombination centers, contribute to carrier scattering, and create spatial inhomogeneities that can lead to early device failure, one of the most important metrics for metamorphic epitaxial materials is a low TDD. The TDD of commercial substrates is typically very low for Si, Ge, GaAs, and InP, with specified TDD values of  $\sim 0 \text{ cm}^{-2}$ ,  $< 3 \times 10^2 \text{ cm}^{-2}$ ,  $< 5 \times 10^3 \text{ cm}^{-2}$ , and  $< 6 \times 10^4 \text{ cm}^{-2}$ , respectively.<sup>15–17</sup> While not extensively explored in this issue, it is interesting to note that nitride semiconductors are commonly grown metamorphically on silicon or sapphire; many commercial devices based on nitrides offer high performance despite TDD values exceeding  $10^8 \text{ cm}^{-2}$  in the active region, making them relatively unique compared to other semiconductor material systems.

Accordingly, relaxing strain through misfit dislocations while maintaining low TDD in the device region is the defining challenge of metamorphic growth. The study of misfit dislocations, dislocation interactions, and dislocation motion has seen considerable attention in II–VI, III–V, and SiGe material systems.<sup>14,18–20</sup> Three primary approaches to reducing the TDD have emerged: abrupt interfaces, buffer layers, and structured interfaces; each has seen a different level of success in different material systems.<sup>4,12,21–27</sup>

An abrupt interface is an atomically abrupt transition from the substrate material to the thin-film layer that is overgrown.

This approach has seen success in the growth of dissimilar III–V semiconductors as the growth conditions have been optimized to facilitate the formation of misfit dislocations. In the literature, dislocation densities of abrupt interfaces have been reported to be below  $1 \times 10^7 \text{ cm}^{-2}$ .<sup>25</sup> The x-ray diffraction (XRD) full width at half maximum for reciprocal space maps of two perfect crystals coherently joined through an array of dislocations was evaluated theoretically, and it was shown that  $60^\circ$  mixed character threading dislocations have a different XRD spot shape than  $90^\circ$  pure-edge misfit dislocations.<sup>28</sup> While this diffraction spot shape is thickness dependent, the aspect ratio of the elliptical shape was determined to be independent of the sample thickness and therefore, can be used to assess the relative degree to which strain is accommodated by the  $90^\circ$  misfit dislocations.<sup>26</sup>

The XRD width of abrupt metamorphic III–V semiconductors can be very narrow, as shown in **Figure 3a**, and high-quality devices have been fabricated by a number of research groups. A cartoon of a rigid model abrupt interface depicting strain relaxation through a periodic array of misfit dislocations aligned to the [110] direction is shown in **Figure 3b**. The distance between misfit dislocations is determined by the ratio of the Burgers vector and the misfit strain between the thin film and substrate. It is common for either strained superlattices<sup>29</sup> or quantum dot structures<sup>27</sup> to be included in device heterostructures to act as dislocation filtering structures that reduce the TDD penetrating the device layers.

Compositionally graded buffer layers have been heavily investigated for achieving high strain relaxation while maintaining low TDD. The basic premise of a graded buffer is to maximize dislocation glide velocity and minimize dislocation nucleation, thus allowing each threading dislocation to do maximum work (i.e., glide very long lengths). **Figure 4** illustrates the dislocation network created through one particular design of a compositionally graded buffer with a cartoon and cross-sectional transmission electron micrograph. The strategy attempts to maintain a low density of glissile threads while minimizing any kinetic barriers to dislocation glide, such as compositional inhomogeneity or excessive surface roughness. While compositionally graded buffers can be very effective in producing dislocation densities as low as  $10^4$ – $10^6 \text{ cm}^{-2}$ ,<sup>22,30</sup> they often require several micrometers of thickness and come with significant surface roughening in the form of crosshatch roughness.

Structured or patterned interfaces make up the last broad class for manipulating dissimilarities in structure between the substrate and thin film. The involved techniques for creating these interfaces include selective area growth, where growth occurs on a pedestal or rib such that the dislocations are able to terminate at a free sidewall before the device region is grown.<sup>21,23,24</sup> **Figure 5** illustrates InP grown selectively on a 300-mm-diameter Si in nanoscale trenches.<sup>24</sup> These techniques are being advanced in facilities combining growth and nano-fabrication capabilities to create metamorphic materials in a deterministic fashion.

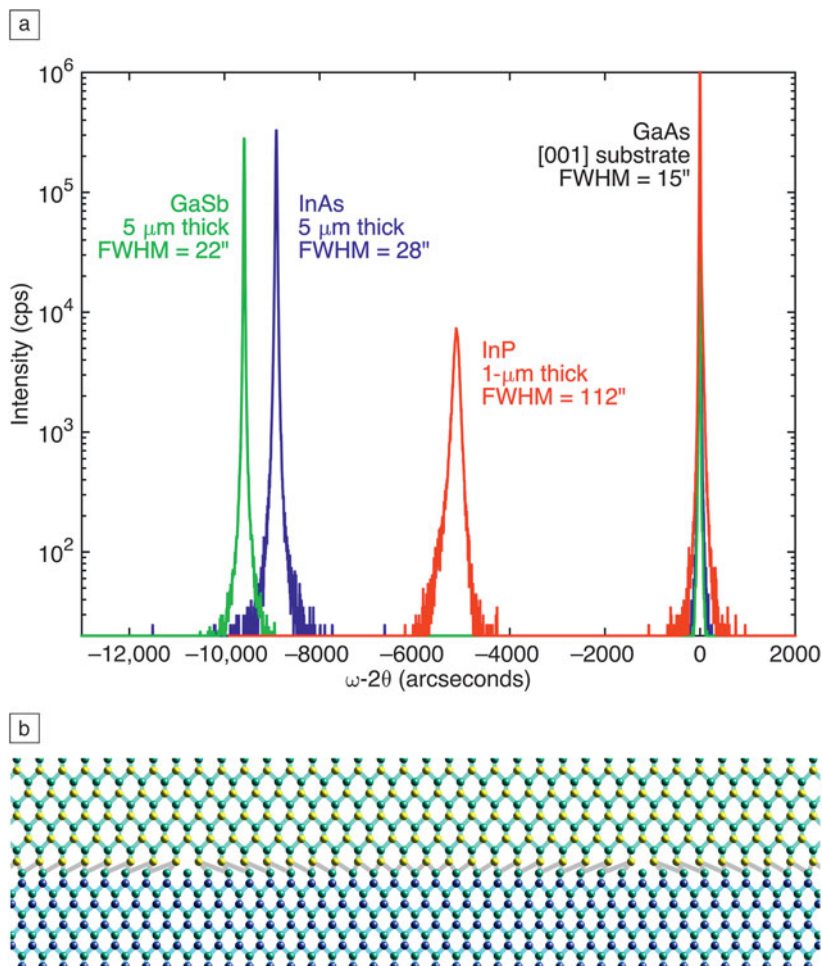


**Figure 3.** (a) Graph of 004 x-ray diffraction peaks of several abrupt metamorphic III–V semiconductors. Adapted with permission from Reference 26. © 2011 American Institute of Physics. Note: FWHM, full width at half maximum; the x-ray diffractometer angle designations for the sample,  $\omega$ , and detector,  $\theta$ , and intensity recorded in counts per second. (b) A rigid model cartoon showing an abrupt metamorphic interface between two III–V compound semiconductors looking down the [110] direction. The green balls represent the Group III atom, and blue and yellow balls represent different Group V atoms that result in significantly different lattice constants of the film and substrate. The substrate bonds are shown in blue, the film bonds in green, and the highly distorted interface bonds in gray. The misfit dislocation lines lie perpendicular to this view, aligned with the green atoms that are depicted with no bonds.

### Common metamorphic epitaxial thin-film growth techniques

Metamorphic epitaxial materials have been grown using a variety of techniques, each tailored to the specific material system. Chemical vapor deposition (CVD) uses gaseous precursors and a thermally driven reaction at the substrate surface to grow material. CVD is widely applied in industry and has been used for both SiGe and III–V compound semiconductor materials, including GaN. The relatively fast growth rate ( $\sim 3\text{--}10 \mu\text{m/h}$ ) is an attractive attribute for growing linearly graded buffers that are conventionally designed to mitigate 1% strain per micrometer of buffer.<sup>5</sup>

Molecular beam epitaxy (MBE), a highly precise form of physical vapor deposition, has been the other major technique

used in metamorphic materials research. While best known as a research tool, MBE is used commercially for the growth of amplifiers for cell phones and wireless devices, as well as laser diodes. In MBE, atomic or molecular beams are generated via effusion cells, electron-beam evaporators, or even pulsed lasers and directed toward a heated substrate in an ultra-high vacuum environment. Hybrid techniques are also possible, where beam fluxes are generated from hydride or metallorganic gas precursors (i.e., gas-source MBE and chemical beam epitaxy).<sup>5</sup>

The relative success of a growth technique typically depends on the thermodynamic and kinetic processing windows of the final material. Accessible growth rate and operating temperatures have a significant impact on these quantities, and the system parameters that are expressed as a strength in one materials system can translate into a weakness in another material. As an example, most MBE systems employ a relatively low growth rate (typically 1–2  $\mu\text{m/h}$ ), which is a disadvantage for growing buffer layers. But precise flux control of MBE facilitates growth of materials that are very sensitive to the V/III ratio, such as III–antimonide compounds.<sup>5,10</sup> In general, all modes of growth technologies—from liquid-phase epitaxy to hydride vapor-phase epitaxy—have opportunities to contribute to developing novel metamorphic epitaxial materials.

### Record-setting performance

In several technology areas, metamorphic epitaxial materials provide state-of-the-art performance. For example, in photovoltaics, metamorphic multijunction solar cells have set many records for efficiency over the past 10 years. The design freedom that metamorphic materials enable allows device designers

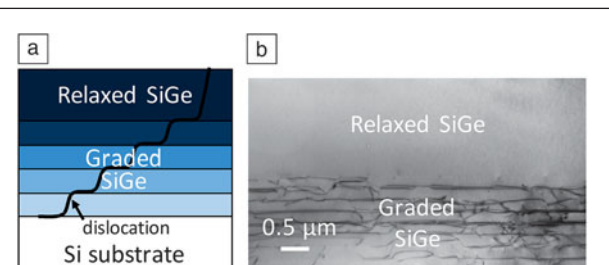


**Figure 4.** (a) Schematic and (b) bright-field transmission electron microscope image of compositionally graded SiGe buffer layer on Si, where threading dislocations may be “recycled” at many mismatched interfaces.

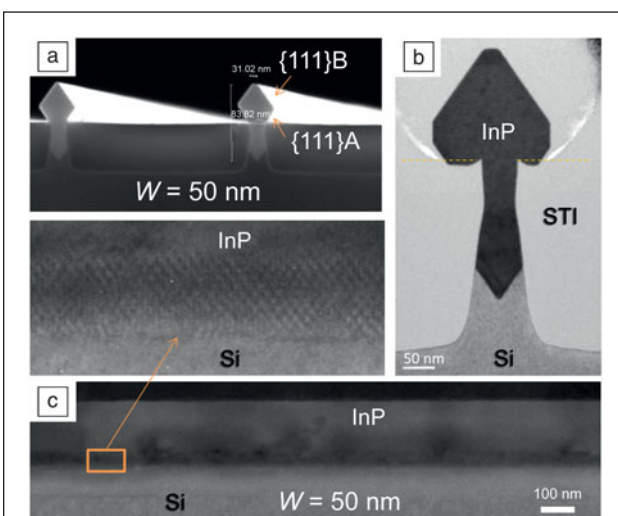


**Figure 5.** InP/Si heterostructure grown in “v-grooved” 50-nm-width trenches with optimized nucleation conditions: (a) (upper) Tilted view scanning electron microscope image and (lower) high-magnification cross-sectional transmission electron microscope image of the orange box area in (c). (b) Perpendicular view showing a twinned region at the InP/Si interface. (c) Parallel view showing a very uniformly grown and low-defect density InP layer with Moiré fringes at the InP/Si bottom interface in inset. {111}A denotes In-terminated plane and {111}B denotes P-terminated plane. Reproduced with permission from Reference 24. © 2014 American Institute of Physics. Note: *W*, trench width.

to tailor the bandgap of the absorbing layers to match the solar spectrum better than what is possible through lattice-matched designs. Most recently, a 45.7%-efficient four-junction concentrator solar cell with two metamorphic junctions was demonstrated;<sup>31</sup> concentrator cells are typically <40% efficient.<sup>32</sup> The future of metamorphic solar cells may lie in the integration of III–V materials with Si, enabling high-efficiency and low-cost solar cells for 1-sun or low-concentration applications. High-efficiency metamorphic solar cells are currently under active commercial development for space applications. In this issue, France et al. discuss the importance of metamorphic materials in both ultrahigh-efficiency devices that operate with efficiencies that are beyond the current commercial state of the art, and in low-cost, high-efficiency solar cells with theoretical efficiencies near 40%.

Metamorphic transistors may soon become important for applications in electronics that push higher performance and higher energy efficiency beyond the capabilities of silicon. It is possible that the complementary metal oxide semiconductor industry will move toward metamorphic nonplanar 3D multi-gate field-effect transistor devices for next-generation logic devices such as FinFETs or tri-gate transistors. Metamorphic transistors may also drive the capabilities of high-speed, mixed-signal applications and high-power devices, allowing new integrated circuit technologies to impact our electronics infrastructure. In their article, Lee and Fitzgerald discuss how these integrated circuits of the future are expected to impact applications in wireless communication, power electronics,

and smart systems that could be used in solid-state lighting, printing, displays, and appliance computing.

Advances in metamorphic semiconductor lasers will include both quantum-well and quantum dot active regions to reach new wavelength regimes using semiconductor devices. Metamorphic III–V lasers on Si may also serve as a critical enabler for Si-integrated photonics, where high-performance digital logic and high-speed optical communication are intimately coupled. Tournié et al. review current progress and the future promise of metamorphic lasers.

## Opportunities and outlook

The final article in this issue by Deelman et al. discusses the applications of metamorphic materials in the area of quantum computing, currently one of the most challenging and exciting areas of research. Precise strain engineering of silicon quantum wells on metamorphic SiGe is needed to remove the conduction-band degeneracy such that electrons occupy only one valley. In addition, low-loss superconducting materials and novel superconductor/semiconductor epitaxial nanowires are being created from metamorphic epitaxial materials that may help propel quantum computing out of the research laboratory. This article reviews the challenges and materials progress toward creating quantum-bit (qubit) devices for quantum information applications that hold promise for ultrafast computation and unbreakable cryptography.

We hope that this issue will help materials scientists and engineers as well as those who use advanced materials to create devices, circuits, and systems to understand how new engineered, single-crystal semiconductor materials offer new opportunities. Technological value resides in the increased design freedom that results from relaxing the requirement that device layers be lattice-matched to a commercially available substrate; metamorphic growth allows essentially all of the space on Figure 2 to be used in device design and may facilitate epitaxial growth of other materials that are not shown. Already, the advantage of this increased design space has produced devices that have set new performance records and are moving toward commercial relevance.

## References

1. K. Eng, T.D. Ladd, A. Smith, M.G. Borselli, A.A. Kislev, B.H. Fong, K.S. Holabird, T.M. Hazard, B. Huang, P.W. Deelman, I. Milosavljevic, A.E. Schmitz, R.S. Ross, M.F. Gyure, A.T. Hunter, *Sci. Adv.* **1** (4), e1500214 (2015).
2. R.M. France, J.F. Geisz, I. Garcia, M.A. Steiner, W.E. McMahon, D.J. Friedman, T.E. Moriarty, C. Osterwald, J.S. Ward, A. Duda, M. Young, W.J. Olavarria, *IEEE J. Photovolt.* **5** (1), 432 (2015).
3. M.L. Lee, E.A. Fitzgerald, M.T. Bulsara, M.T. Currie, A. Lochtefeld, *J. Appl. Phys.* **97**, 011101 (2005).
4. T. Wang, H. Liu, A. Lee, F. Pozzi, A. Seeds, *Opt. Express* **19** (12), 11381 (2011).
5. T.F. Kuech, Ed., *Handbook of Crystal Growth: Thin Films and Epitaxy* 2nd ed. (Elsevier, Amsterdam, The Netherlands, 2015), vol. 3A.
6. Z. Alferov, *Rev. Mod. Phys.* **74**, 767 (2001).
7. H. Kroemer, *Rev. Mod. Phys.* **73** (3), 783 (2001).
8. N. Holonyak, *Proc. IEEE* **85** (11), 1678 (1997).
9. H. Rupprecht, J.M. Woodall, G.D. Pettit, *Appl. Phys. Lett.* **11** (3), 81 (1967).

10. R.F.C. Farrow, R.F. Bunshah, G.E. McGuire, Eds., *Molecular Beam Epitaxy: Application to Key Materials*, Materials Science and Process Technology Series, (Noyes Publications, Park Ridge, N.J. 1995).
11. S.R. Bank, M.A. Wistey, L.L. Goddard, H.B. Yuen, V. Lordi, J.S. Harris, *IEEE J. Quantum Electron.* **40**, 656 (2004).
12. G. Belenky, L. Shterengas, D. Wang, G. Kipshidze, L. Vorobjev, *Semicond. Sci. Technol.* **24**, 115013 (2009).
13. N. Tansu, L.J. Mawst, *IEEE Photon. Technol. Lett.* **13** (3), 179 (2001).
14. J.W. Matthews, *J. Vac. Sci. Technol.* **12**, 126 (1975).
15. <http://www.sunedisonsemi.com/index.php?view=perfect-silicon&l1=25&l2=47>.
16. <http://www.wafertech.co.uk/products/indium-phosphide-inp>.
17. <http://www.axt.com/site/index.php?q=node/34>.
18. R.S. Goldman, K.L. Kavanagh, H.H. Wieder, S.N. Ehrlich, R.M. Feenstra, *J. Appl. Phys.* **83**, 5137 (1998).
19. J.E. Ayers, *Heteroepitaxy of Semiconductors: Theory, Growth, and Characterization* (CRC Press, New York, 2007).
20. E.A. Fitzgerald, *Mater. Sci. Rep.* **7** (3), 91 (1991).
21. E.A. Fitzgerald, G.P. Watson, R.E. Proano, D.G. Ast, P.D. Kirchner, G.D. Pettit, J.M. Woodall, *J. Appl. Phys.* **65**, 2220 (1989).
22. E.A. Fitzgerald, Y.-H. Xie, M.L. Green, D. Brasen, A.R. Kortan, J. Michel, Y.-J. Mii, B.E. Weis, *Appl. Phys. Lett.* **59**, 811 (1991).
23. J.Z. Li, J. Bai, J.-S. Park, B. Adekore, K. Fox, M. Carroll, A. Lochtefeld, Z. Shellenbarger, *Appl. Phys. Lett.* **91**, 021114 (2007).
24. C. Merckling, N. Waldron, S. Jiang, W. Guo, N. Collaert, M. Caymax, W. Vandervorst, *J. Appl. Phys.* **115**, 023710 (2014).
25. C.J.K. Richardson, L. He, P. Apiratikul, N.P. Siwak, R.P. Leavitt, *Appl. Phys. Lett.* **106**, 101108 (2015).
26. C.J.K. Richardson, L. He, S. Kanakaraju, *J. Vac. Sci. Technol. B* **29** (3), 03C126 (2011).
27. J. Yang, P. Bhattacharya, Z. Mi, *IEEE Trans. Electron Devices* **54** (11), 2849 (2007).
28. V.M. Kaganer, R. Köhler, M. Schmidbauer, R. Opitz, B. Jenichen, *Phys. Rev. B* **55** (3), 1793 (1997).
29. K. Nozawa, Y. Horikoshi, *Jpn. J. Appl. Phys.* **30** (4b), L668 (1991).
30. K.E. Lee, E.A. Fitzgerald, *J. Cryst. Growth* **312** (2), 250 (2010).
31. [http://www.nrel.gov/ncpv/images/efficiency\\_chart.jpg](http://www.nrel.gov/ncpv/images/efficiency_chart.jpg).
32. G.S. Kinsey, "Spectrum Sensitivity, Energy Yield, and Revenue Prediction of PV and CPV Modules," presented at the 42nd IEEE Photovoltaic Specialist Conference (PVSC), New Orleans, June 14–19, 2015.
33. J. Schöne, "Kontrolle von Spannungsrelaxation und Defektbildung in Metamorphen III–V Halbleiterheterostrukturen für Hocheffiziente Solarzellen," PhD thesis, Christian-Albrechts-Universität, Kiel, Germany (2009). □

**MRS OnDemand® WEBINAR SERIES**

Register at [www.mrs.org/webinars](http://www.mrs.org/webinars)

April 20, 2016 | 11:00 am – 12:00 pm (ET)

**Twinning in Metallic Materials: Strengthening and Plasticity**

Presented by: **MRS Bulletin**

# High Resolution RBS

National Electrostatics Corporation has added Ångstrom level, High Resolution RBS to the RC43 Analysis System for nanotechnology applications. A single Pelletron instrument can now provide RBS, channeling RBS, microRBS, PIXE, ERDA, NRA, and HR-RBS capability, collecting up to four spectra simultaneously.

Pelletron accelerators are available with ion beam energies from below 1 MeV in to the 100 MeV region.

[www.pelletron.com](http://www.pelletron.com)  
 Phone: 608-831-7600  
 E-mail: [nec@pelletron.com](mailto:nec@pelletron.com)

Full wafer version of the model RC43 analysis end station with High Resolution RBS Detector.



**National Electrostatics Corp.**

MRS Booth 213